Supplemental material

Supplemental Experimental Procedure

Quantification of cell-cell junctional localization. The membranous localization of ectopically expressed EGFP-fusion proteins was determined by measuring the distribution of fluorescent intensity across two neighboring cells with NIH image-J 1.43r (36). The average fluorescent intensity of each fusion protein was determined from at least six separate cell-cell junctions in more than three independent experiments. For normalization, the minimum fluorescent intensity from each line was subtracted from the measured value to set the base line fluorescence at 0%. The resulting value was divided by the maximum adjusted value of measured intensity (100%) to obtain an overall distribution of fluorescent intensity across each junction.

Supplemental Figure Legends

Supplemental Fig. S1 A: Expression of the N-myristoylation peptide-tagged C-PMT WT and C-PMT ΔC1(4H) WT in 293T cells. 293T cells were transfected with the indicated C-PMT variants and cell lysate after a 24-h transfection was subjected to SDS-PAGE and western blotting. Recombinant C-PMT (50 ng/lane) was used as a positive control of each experiment. Representative results are shown. The relative amount of each protein was derived from the intensity of the band of each protein by using densitometry compared to C-PMT WT (C-PMT WT = 1). NM: the N-myristoylated peptide-tag (MGSSKSKPKVSN), G2A: an unmyristoylated analogue of NM, in which the second residue glycine is replaced by alanine. B: Western blotting of recombinant proteins in the HVJ-liposome. Each 8.75 μl of the HVJ-liposomes containing recombinant proteins was subjected to 7.5% SDS-PAGE and visualized by using rabbit anti-PMT (23). One micro gram of C-PMT WT was used as a positive control.

Supplemental Fig. S2 Intracellular localization of C-PMT WT and C-PMT ΔC1(4H) in CHO-K1 cells. C-PMT, and C-PMT ΔC1(4H) were expressed in CHO-K1 cells and located by fluorescence microscopy (green). The nucleus was visualized with DAPI (blue). Images are presented at the same magnification. (Scale bar: 10 μm.)

Supplemental Fig. S3 The average percentage of the C-PMTs expressed in the membranous fraction. Six independent experiments were carried out as described in Fig. 2C, and the intensity of each band of C-PMT WT and C-PMT ΔC1(4H) was determined by densitometry. The value of the % membranous fraction was obtained by dividing the densitometric value of each band in the membranous fraction by the sum of the densitometric values of the corresponding bands in both the cytosolic and membranous fractions. Each bar represents the mean + s.d. for six experiments. Student's *t* test was employed to determine the statistical significance of the difference in amounts of the membranous fraction between C-PMT WT and C-PMT ΔC1(4H). *: significantly different ($P<0.05$).

Supplemental Fig. S4 C1(4H)-EGFP and TcdB(N4H)-EGFP localize to the plasma membrane of 293 cells. A: Intracellular localization of C1(4H)-EGFP and TcdB(N4H)-EGFP. C1(4H)-EGFP and TcdB(N4H)-EGFP were expressed in 293 cells and located by fluorescence microscopy (green, upper panel). The plasma membrane region was visualized with anti-human CD46 antibody (red, lower panel). Images are presented at the same magnification. B: The normalized fluorescent intensity of cell-cell junction (white line in panel A) was determined by ImageJ as described in Supplemental Experimental Procedure. Closed circles represent EGFP-derived fluorescence (green in Fig. S4A) and open circles represent CD46-derived fluorescence (red in Fig. S4A) Left: C1(4H)-EGFP, middle: EGFP, right: TcdB(N4H)-EGFP. C: Fluorescent intensity of cell-cell junctions from three constructs (left: C1(4H)-EGFP, middle: EGFP, right: TcdB(N4H)-EGFP). The fluorescent intensity at at least two cell-cell junctions in each experiment was measured by Image-J (n=7 to 14). The fluorescent intensity of EGFP and CD46 is

shown in the upper panel and lower panel, respectively. Each color represents the measurement of each cell-cell junction. D: The average fluorescent intensity measurement of cell-cell junctions obtained from the results shown in Fig. S4C. Closed circles represent EGFP-derived fluorescence and open circles represent CD46-derived fluorescence.

Supplemental Fig. S5 Intracellular localization of the C1(4H)-EGFP variants. The C1(4H)-EGFP variants expressed in 293 cells and were located by fluorescence microscopy (green). The plasma membrane was visualized by using anti-human CD46 antibody (red). The images are presented at the same magnification. (Scale bar: 10 μm.)

Supplemental Fig. S6 A: Fluorescent intensity at cell-cell junctions from C1(4H)-EGFP and its variants. At least two cell-cell junctions in each experiment were subjected to measurements of fluorescent intensity by Image-J (n=7 to 14). Each color represents the measurement of each cell-cell junction. B: The average fluorescent intensity of cell-cell junctions was obtained from the data shown in panel A.

Supplemental Fig. S7 Cellular localization of the N-myristoylation peptide-tagged C-PMT WT and C-PMT ΔC1(4H) in 293T cells. Each protein was expressed in 293T cells and located by fluorescence microscopy (green). The plasma membrane region was visualized with anti-human CD46 antibody (red). Images are presented at the same magnification. (Scale bar: 10 μm.) NM: the N-myristoylated peptide-tag, G2A: an unmyristoylated analogue of NM.

Supplemental Fig. S8 Effect of the N-myristoylation peptide-tagged C-PMT ΔC1(4H) on the NFAT-luciferase assay of 293T cells. The data on luciferase activity obtained from the experiments in Fig. 6 were normalized to the densitometric values of each band in the western blot analysis shown in Fig. S1A. Each data point represents the mean of at least triplicate measurements. The error bar shows s.d. Representative results from three independent experiments are shown. NM: the N-myristoylated peptide-tag, G2A: an unmyristoylated analogue of NM.

Supplemental Fig. S9 C-PMT interacts with phospholipids through the C1 domain. This surface plasmon resonance (SPR) sensorgram shows that C-PMT but not C-PMT ΔC1(4H) bound to liposomes containing phospholipids. Each protein was analyzed at 500 nM. For the SPR analysis, C-PMT was constructed as described in the experimental procedures and the PMT activity of C-PMT was confirmed by mitogenic activity with HVJ-liposomes (data not shown).

Supplemental Table S1 Primers for construction of plasmids in this study

TABLE S1 Primers for construction of plasmids in this study

Plasmid	Sense primer	Antisense primer
pcDNA3-C1(4H)-EGFP	AAGCTTCaccatggtaagcaatgctaaactattag	AAGCTTaggaagataaagcgctttttc
pcDNA3-TcdB(N4H)-EGFP	GGATCCatgagtttagttaatagaaaacag	AAGCTTaaaatgtaaatttttctcaactgg
pcDNA3-C1(H1)-EGFP	AAGCTTCaccatggtaagcaatgctaaactattag	AAGCTTctttccaataacggaagctcttgc
pcDNA3-C1(H12)-EGFP	AAGCTTCaccatggtaagcaatgctaaactattag	AAGCTTactgttatgtattctttgtagtttggc
pcDNA3-C1(H123)-EGFP	AAGCTTCaccatggtaagcaatgctaaactattag	AAGCTTaggttgcgattcttcataaagatc
pcDNA3-C1(H234)-EGFP	AAGCTTcaccatgcctattggagaatcatataaaa	AAGCTTaggaagataaagcgctttttc
pcDNA3-C1(H34)-EGFP	AAGCTTCaccatgaatatcttagatgagcgacaag	AAGCTTaggaagataaagcgctttttc
pcDNA3-C1(H4)-EGFP	AAGCTTcaccatgtcttcagagcgtttgaatgcttttc	AAGCTTaggaagataaagcgctttttc
pcDNA3-NM-C-PMT WT	GGATCCaccatggggagtagcaagagcaagcctaaggtaagcaatgctaaactattag	gtaccgcatgcctcgagggatcctc
pcDNA3-G2A-C-PMT WT	GGATCCaccatggcgagtagcaagagcaagcctaaggtaagcaatgctaaactattag	gtaccgcatgcctcgagggatcctc
pcDNA3-NM-C-PMTΔC1(4H)	GGATCCaccatggggagtagcaagagcaagcctaaggaaatggaagcattaaaaaaac	gtaccgcatgcctcgagggatcctc
pcDNA3-G2A-C-PMTΔC1(4H)	GGATCCaccatggcgagtagcaagagcaagcctaaggaaatggaagcattaaaaaaac	gtaccgcatgcctcgagggatcctc
pPROEX-1-C-PMTΔC1(4H)	GGATCCaccatggaaatggaagcattaaaaaaac	gtaccgcatgcctcgagggatcctc
pGEX-C1(4H)	GGATCCaccatggtaagcaatgctaaactattag	AAGCTTaggaagataaagcgctttttc

Letters of each primer sequence in upper case are recognition sites for the DNA restriction enzyme.

A

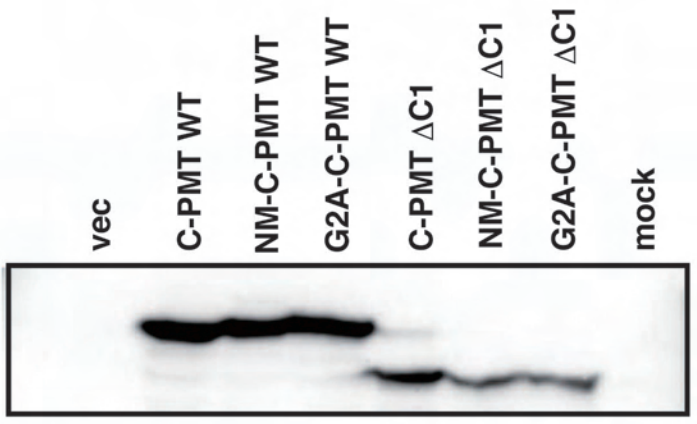

Relative amount	0.0	1.0	0.9	1.0	0.5	0.3	0.4	0.0

B

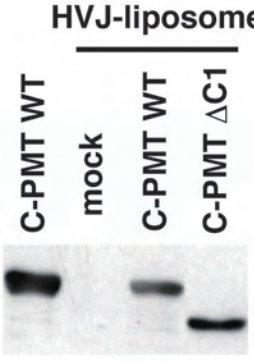

Fig. S1

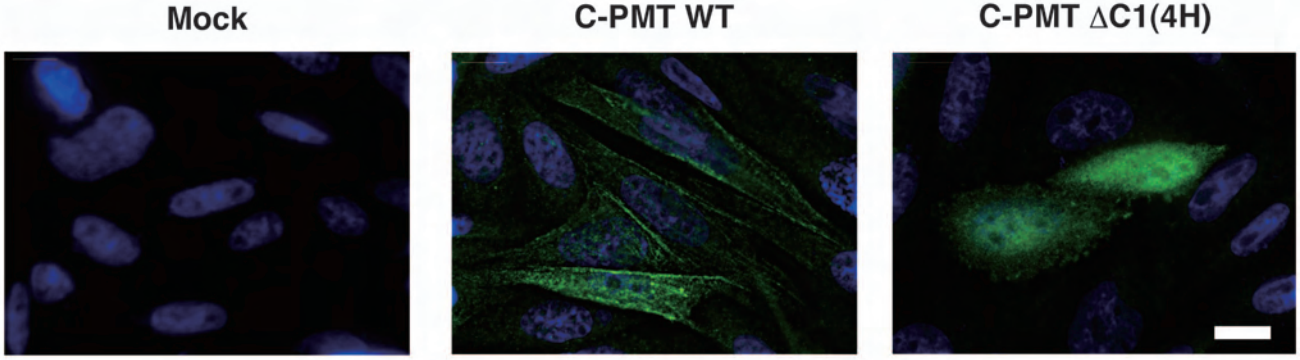

Fig. S2

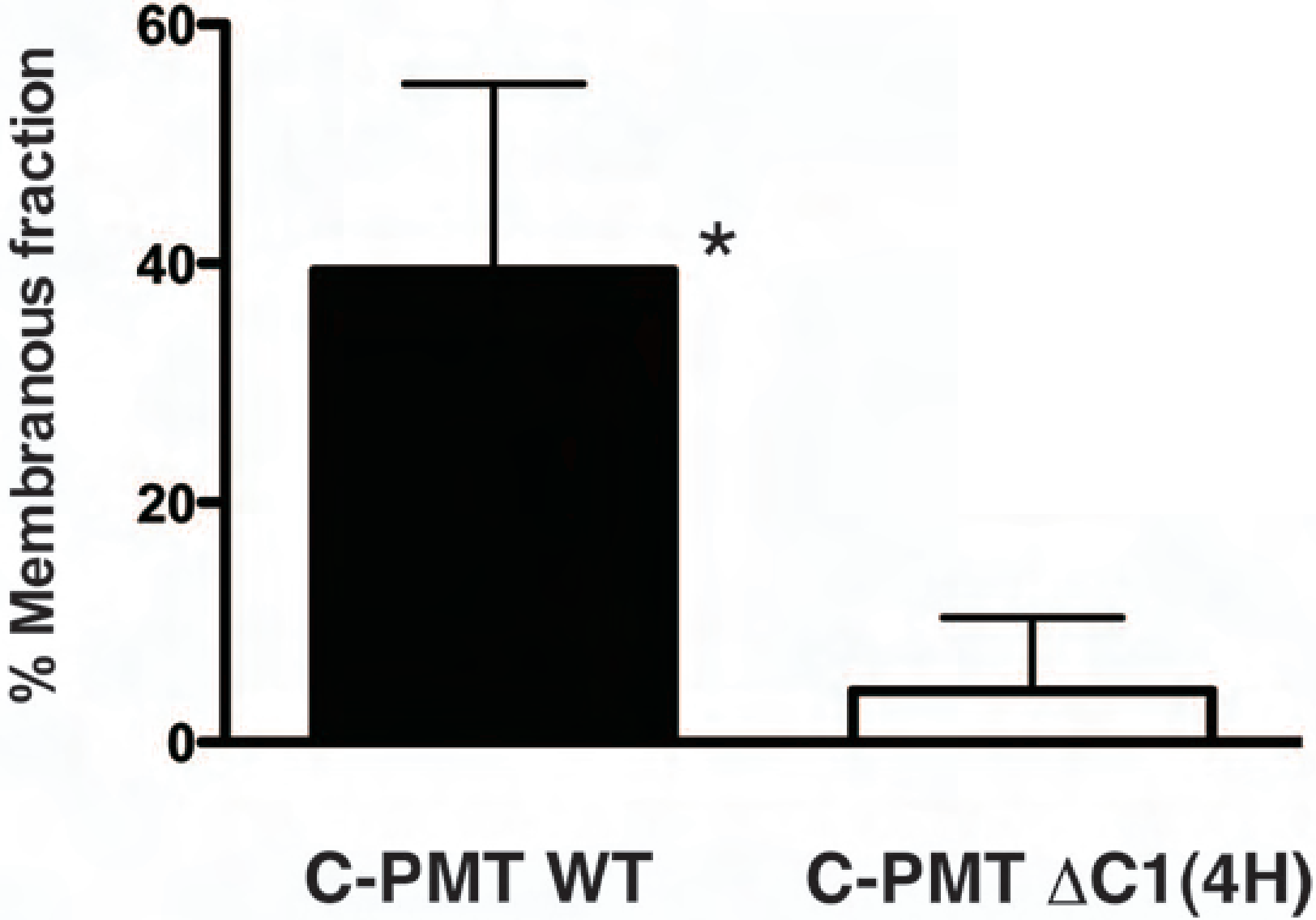

Fig. S3

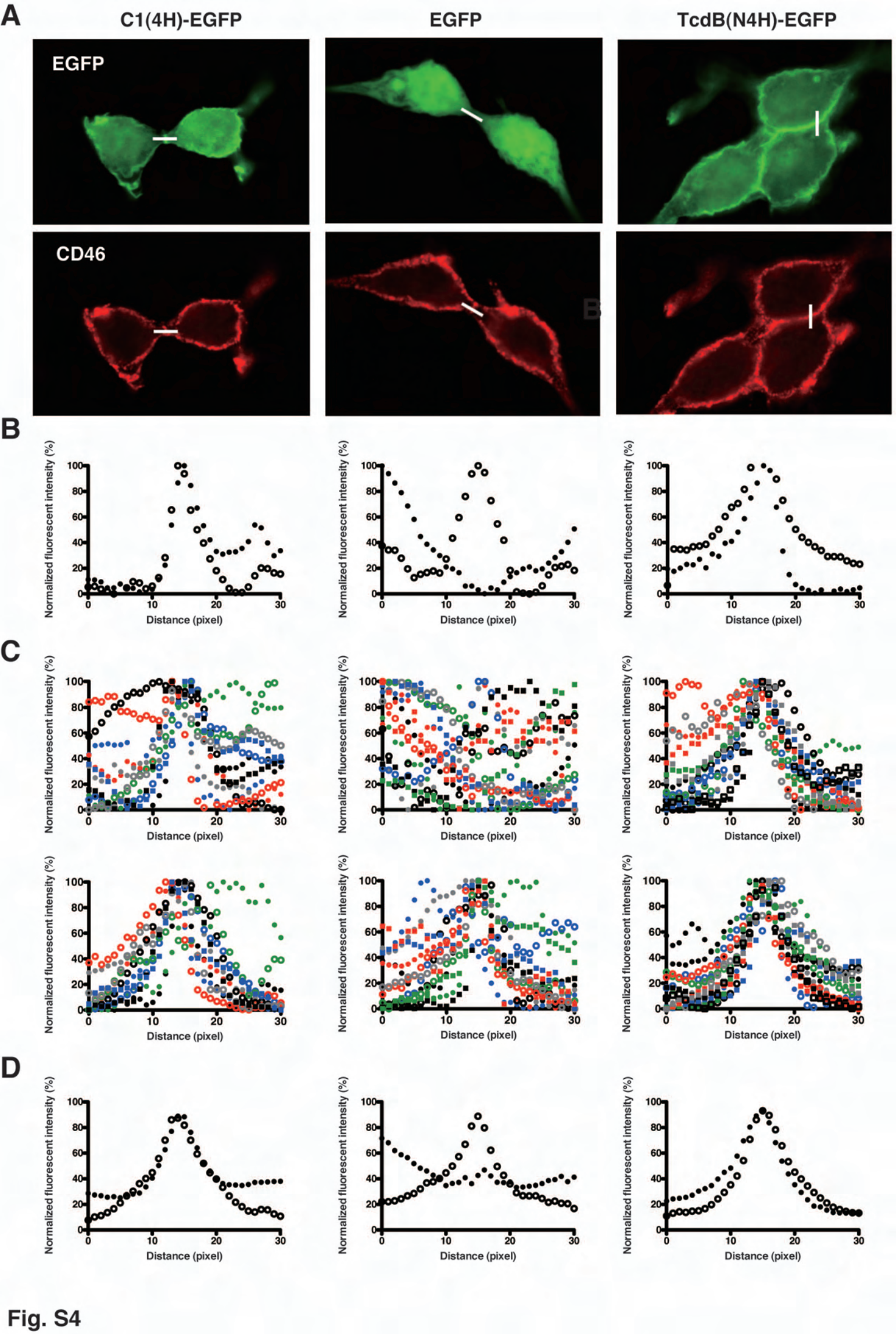
A
C1(4H)-EGFP
EGFP
TcdB(N4H)-EGFP
EGFP
CD46
B
C
D
Normalized fluorescent intensity (%)
Distance (pixel)
0
10
20
30
0
20
40
60
80
100

Fig. S4

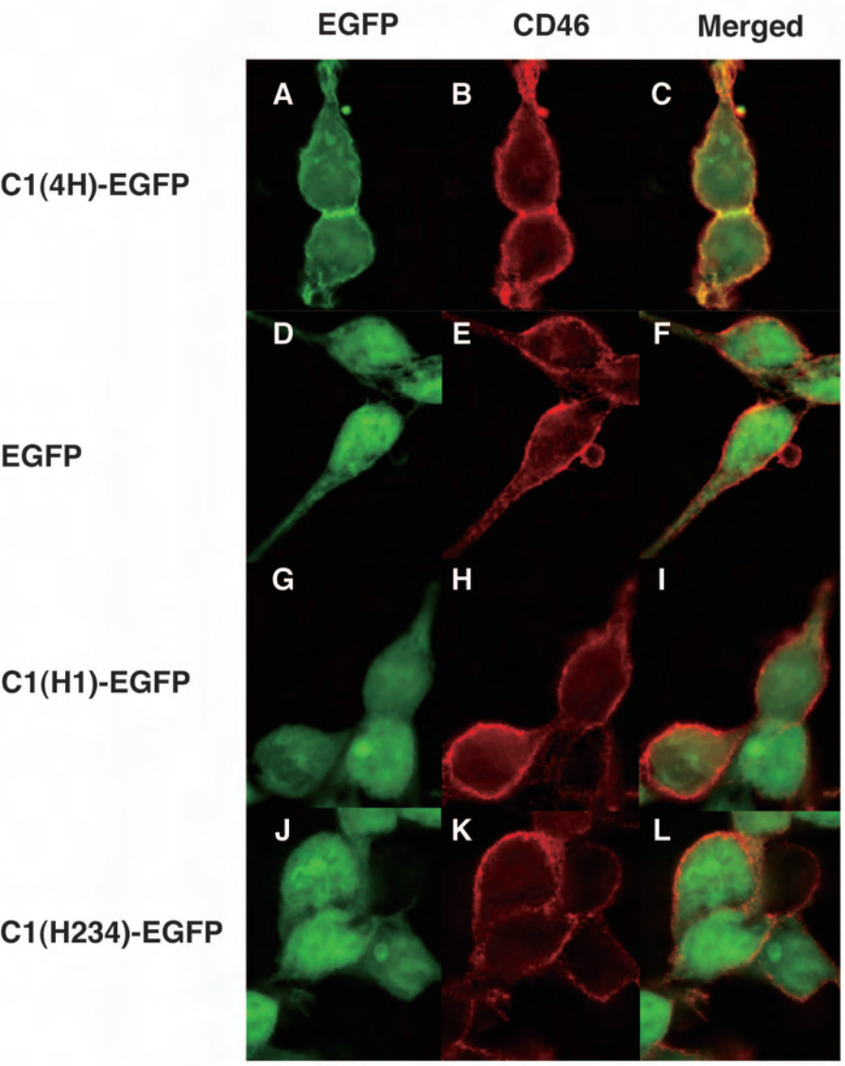
EGFP
CD46
Merged
A
B
C
C1(4H)-EGFP
D
E
F
EGFP
G
H
I
C1(H1)-EGFP
J
K
L
C1(H234)-EGFP

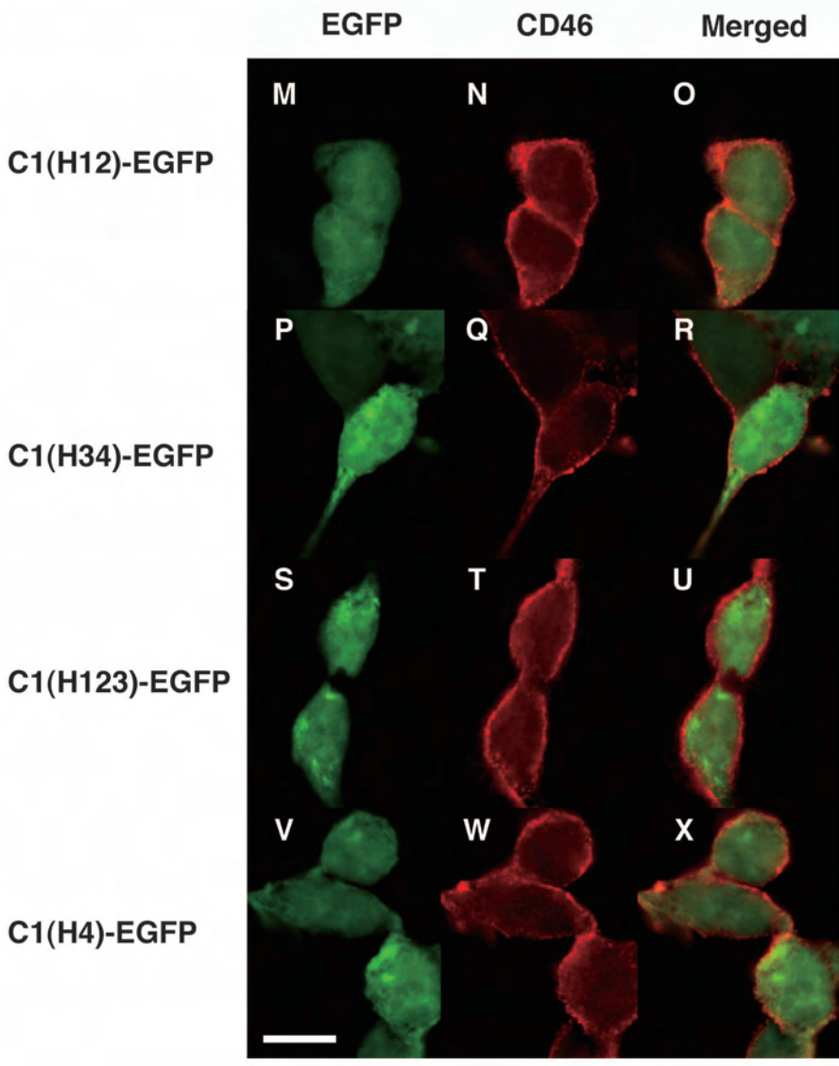
EGFP
CD46
Merged
M
N
O
C1(H12)-EGFP
P
Q
R
C1(H34)-EGFP
S
T
U
C1(H123)-EGFP
V
W
X
C1(H4)-EGFP

Fig. S5

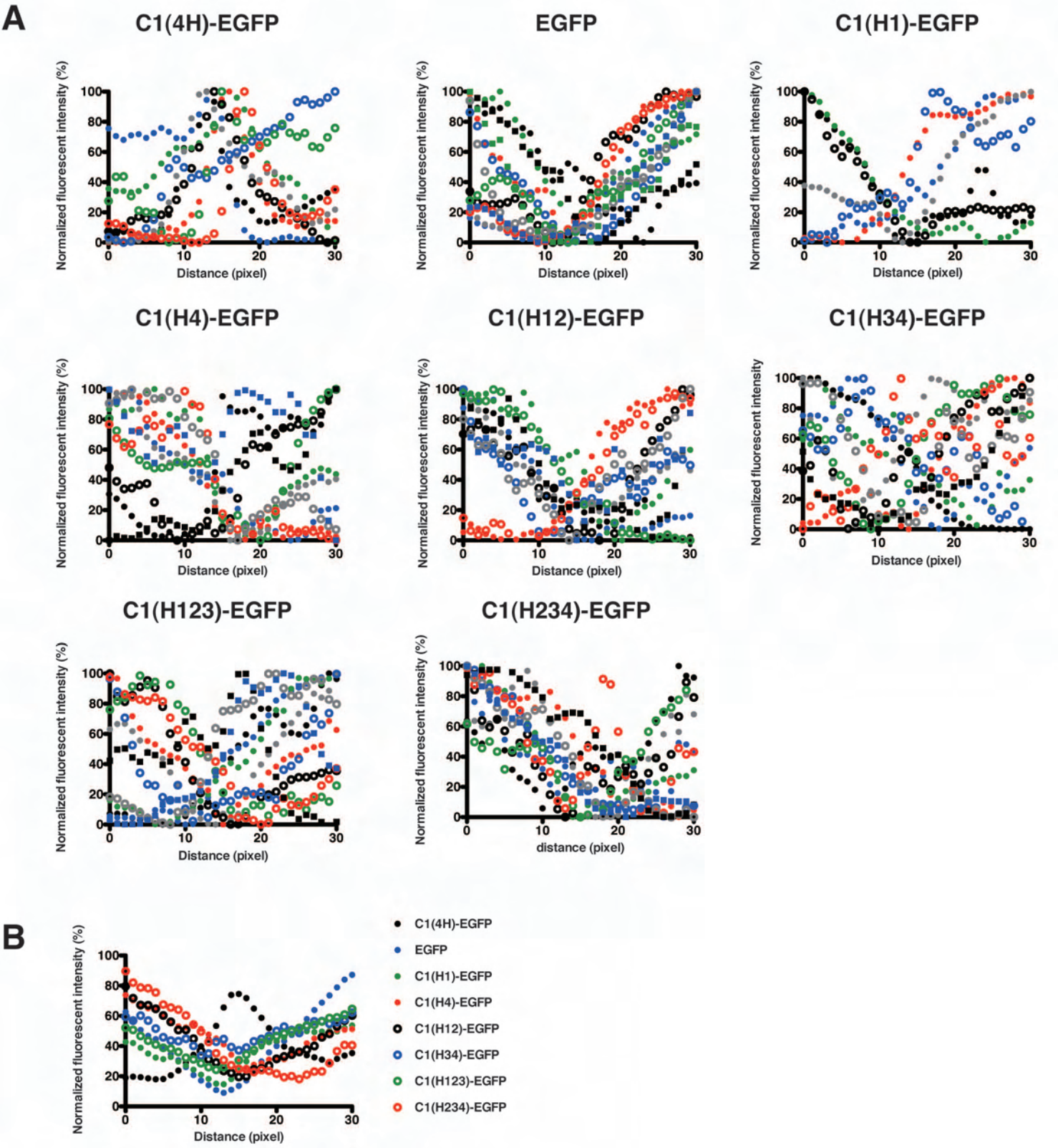
A
C1(4H)-EGFP
EGFP
C1(H1)-EGFP
C1(H4)-EGFP
C1(H12)-EGFP
C1(H34)-EGFP
C1(H123)-EGFP
C1(H234)-EGFP
Normalized fluorescent intensity (%)
Distance (pixel)
distance (pixel)
B
C1(4H)-EGFP
EGFP
C1(H1)-EGFP
C1(H4)-EGFP
C1(H12)-EGFP
C1(H34)-EGFP
C1(H123)-EGFP
C1(H234)-EGFP

Fig. S6

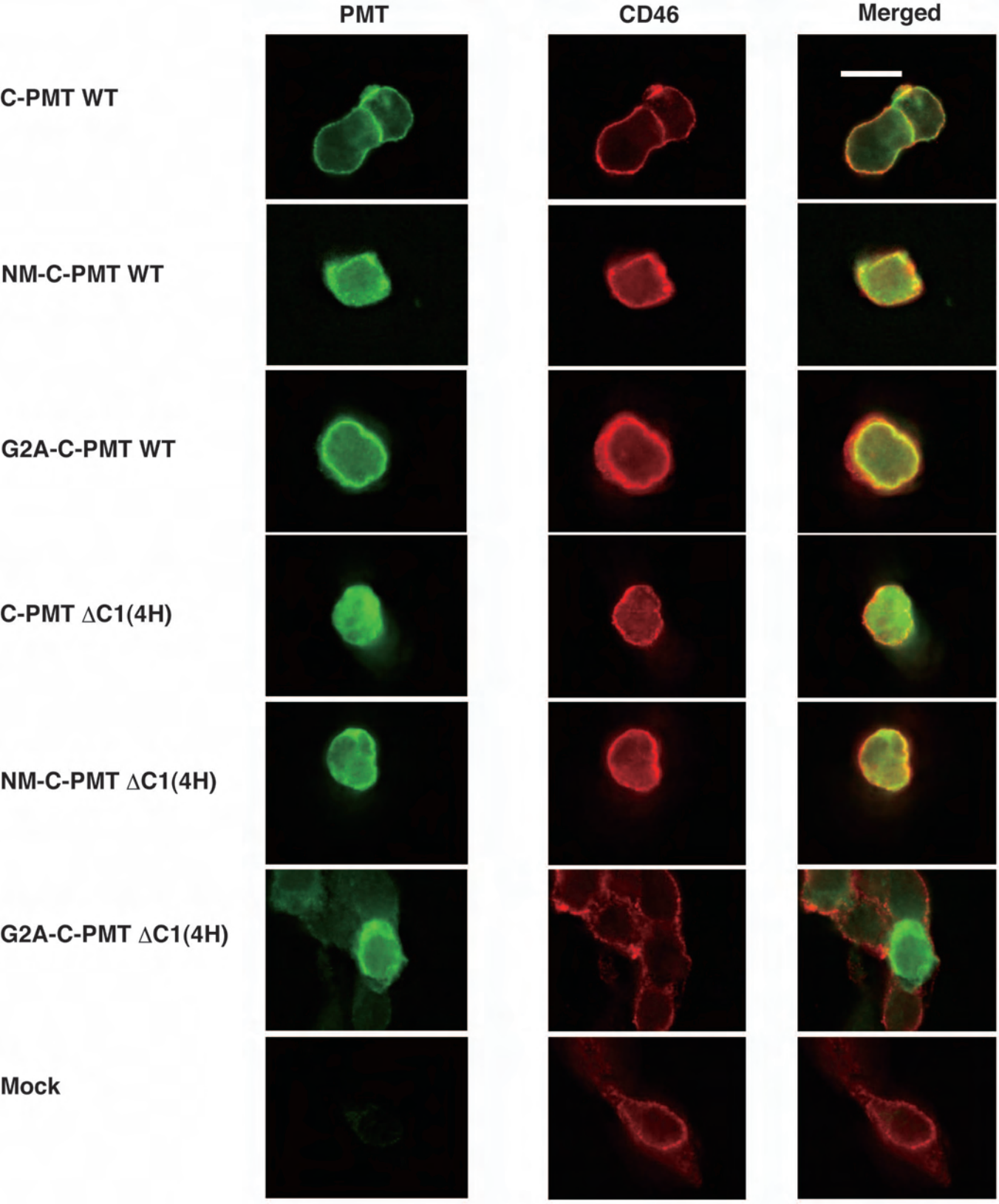
PMT
CD46
Merged
C-PMT WT
NM-C-PMT WT
G2A-C-PMT WT
C-PMT ΔC1(4H)
NM-C-PMT ΔC1(4H)
G2A-C-PMT ΔC1(4H)
Mock

Fig. S7

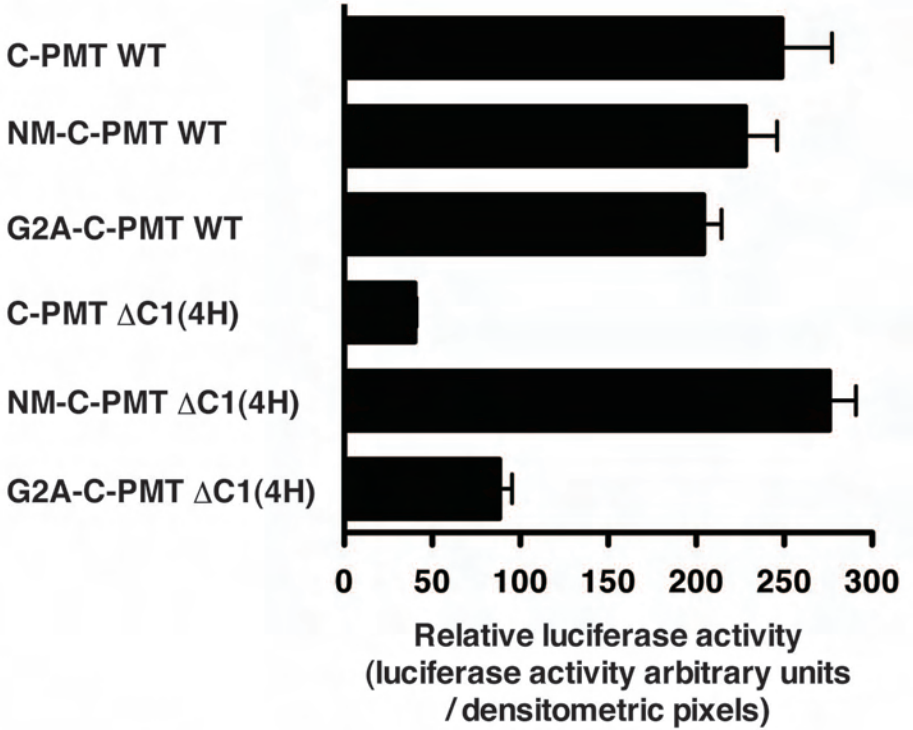
C-PMT WT
NM-C-PMT WT
G2A-C-PMT WT
C-PMT ΔC1(4H)
NM-C-PMT ΔC1(4H)
G2A-C-PMT ΔC1(4H)
0
50
100
150
200
250
300
Relative luciferase activity
(luciferase activity arbitrary units
/ densitometric pixels)

Fig. S8

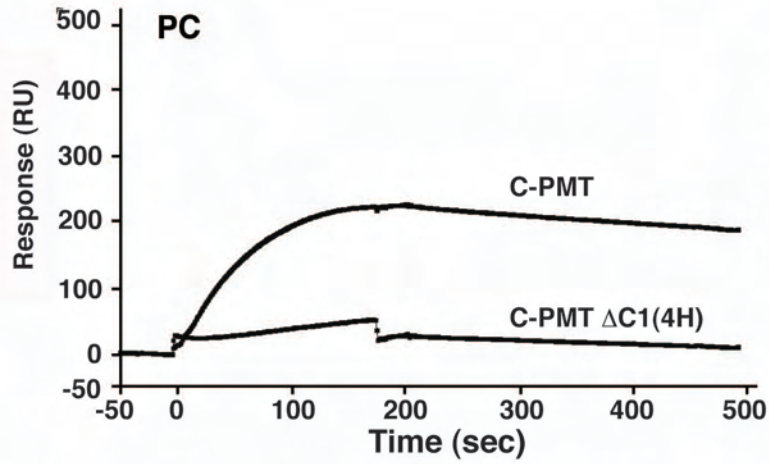
PC
Response (RU)
Time (sec)
C-PMT
C-PMT ΔC1(4H)

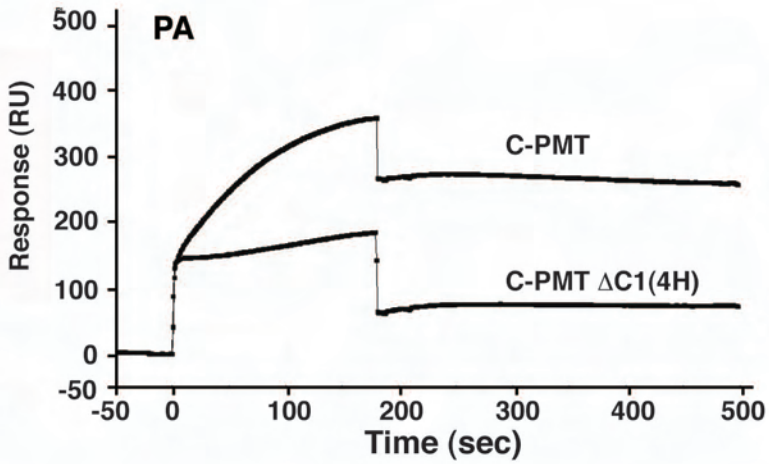
PA
Response (RU)
Time (sec)
C-PMT
C-PMT ΔC1(4H)

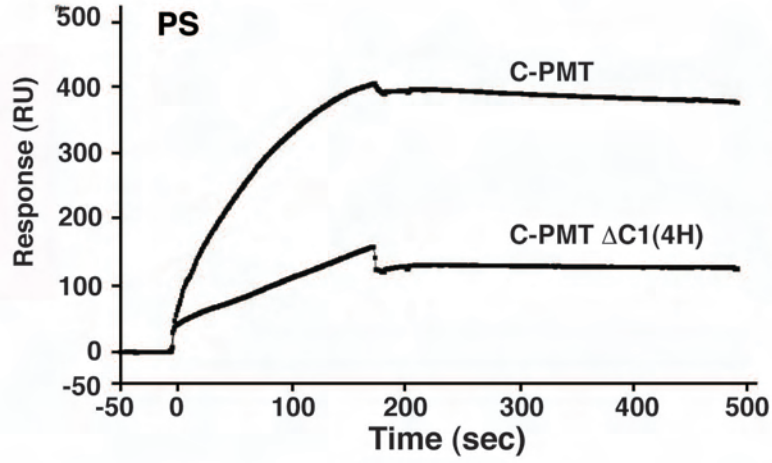
PS
Response (RU)
Time (sec)
C-PMT
C-PMT ΔC1(4H)

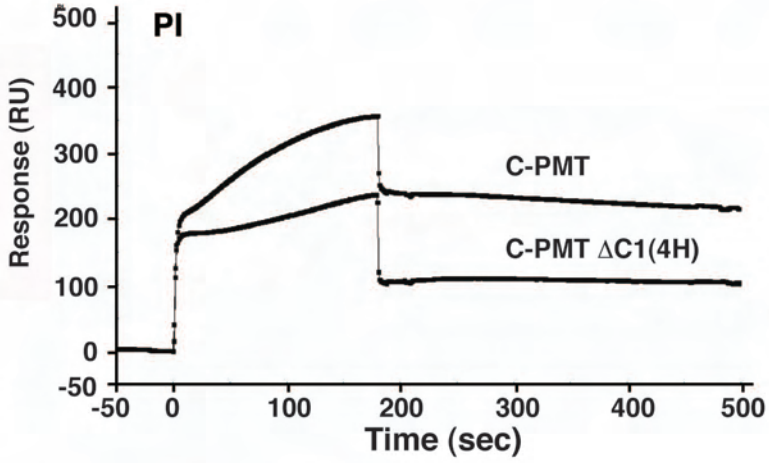
PI
Response (RU)
Time (sec)
C-PMT
C-PMT ΔC1(4H)

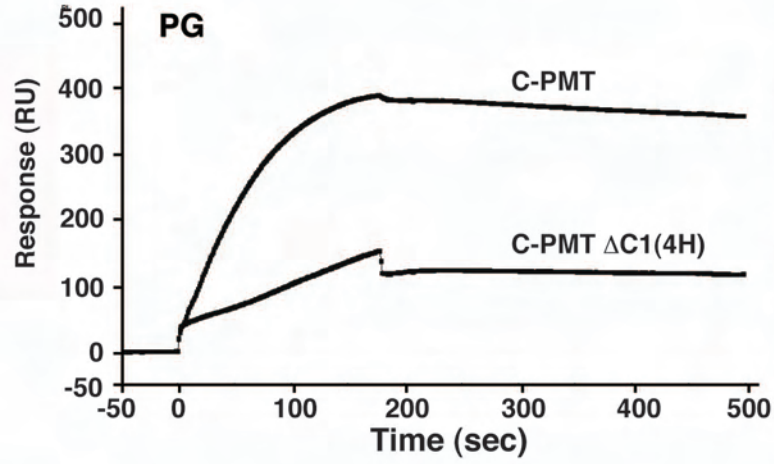
PG
Response (RU)
Time (sec)
C-PMT
C-PMT ΔC1(4H)

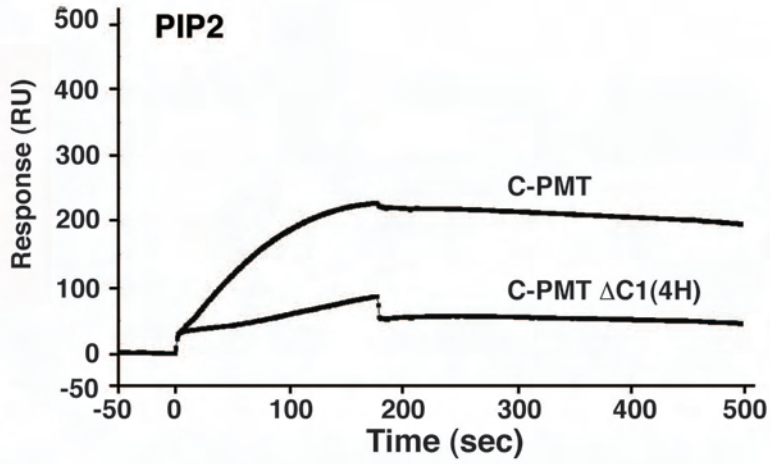
PIP2
Response (RU)
Time (sec)
C-PMT
C-PMT ΔC1(4H)

Fig. S9